Molecular structure and chiral recognition ability of highly branched cyclic dextrin carbamate derivative

Aika Kishimoto,[a] Madoka Mizuguchi,[a] Akiyuki Ryoki,[a,b] and Ken Terao,[*,a]
[a]*Department of Macromolecular Science, Graduate School of Science, Osaka University, 1-1 Machikaneyama-cho, Toyonaka, Osaka 560-0043, Japan*
[b]*Department of Polymer Chemistry, Graduate School of Engineering, Kyoto University, Katsura, Kyoto 615-8510, Japan*
* Corresponding author.
Phone.: +81 6 6850 5459.
E-mail address: terao.ken.sci@osaka-u.ac.jp

ABSTRACT
A hyperbranched polymer, highly branched cyclic dextrin tris(3,5-dimethylphenylcarbamate) (HDMPC), consisting of rigid rodlike subchains was synthesized to investigate dimensional and hydrodynamic properties of HDMPC in methyl acetate and 4-methyl-2-pentanone at 25 °C. Both gyration radii and intrinsic viscosities of the HDMPC sample in the two solvents were much smaller than those for the linear amylose tris(3,5-dimethylphenylcarbamate) (ADMPC) chain with the corresponding molar mass. The chiral column made of the HDMPC sample has chiral separation ability for 8 racemates with a mobile phase of hexane/2-propanol while 6 of them were also separated by our previously investigated linear ADMPC column. These results indicate that HDMPC retains the functionality of the rigid linear ADMPC chain with much smaller chain dimensions and lower solution viscosity than those for the linear chain with the same molar mass.

Keywords: hyperbranched polymers; polysaccharide derivative; chiral stationary phase; small-angle X-ray scattering; chain stiffness

Abbreviations: ADMPC, amylose tris(3,5-dimethylphenylcarbamate); A-silica, 3-aminopropyltriethoxysilane treated silica gel; c, polymer mass concentration; cADMPC, cyclic ADMPC; CSP, chiral stationary phase; $1/C_0$ and $1/C$, number of branching points; CD, circular dichroism; $Đ$, dispersity index; g_s, radius of gyration contraction factor; g_η, intrinsic viscosity shrink factor; HBCD, highly-branched cyclic dextrin; HDMPC, HBCD tris(3,5-dimethylphenylcarbamate); $I(q)$, scattering intensity; k', Huggins constant; k_1 and k_2, capacity factors; L_K, Kuhn segment length; M_0, molar mass of the repeat unit; MALS, multi-angle light scattering; MEA, methyl acetate; MIBK, 4-methyl-2-pentanone; M_w, weight-average molar mass; N, plate number; N_w, weight-average degree of polymerization; $P(q)$, form factor; q, magnitude of the scattering vector; R_g, radius of gyration; SAXS, small-angle X-ray scattering; SEC, size-exclusion chromatography; THF, tetrahydrofuran; V_0, dead volume; V_x, peak retention volume; $\Delta I(q)$, excess scattering intensity; α, separation factor; $[\eta]$, intrinsic viscosity; λ_0, wavelength in a vacuum; Φ, Flory viscosity factor.

Introduction

Highly branched polymers are widely investigated owing to their characteristics including the high segment density, low solution viscosity, and large number of end groups comparing with the corresponding linear polymer (Lederer & Burchard, 2015). Versatile applications were reported as stimuli responsive materials (D. L. Wang, Jin, Zhu, & Yan, 2017), drug or gene delivery carriers (Cook & Perrier, 2020), and templates for mesoporous materials (Bonaccorsi, Calandra, Amenitsch, Proverbio, & Lombardo, 2013). Novel synthesis methods were also developed to obtain well-defined hyperbranched polymers (Chen & Kong, 2016; Hirao & Yoo, 2011; Yamago, 2021). Dimensional and hydrodynamic properties of hyperbranched polymers in solution were thus extensively studied (Burchard, 2004; Hao, Zhu, & Li, 2019; Hirao & Yoo, 2011; Lederer & Burchard, 2015) to clarify their conformational characteristics. Almost all hyperbranched polymers investigated are, however, composed of relatively flexible subchains except for dendrimers with very short subchains probably because of the difficulty to synthesize rigid hyperbranched polymers.

Amylopectin is a highly-branched natural polymer consisting of α-(1-4) linked glucose linear chains that are connected by α-(1-6) branch linkages. While it has wide molar mass distribution, Takata et al. (Takata, Ohdan, Takaha, Kuriki, & Okada, 2003; Takata et al., 1996) revealed that highly-branched cyclic dextrin (HBCD) with relatively narrow distribution of molar mass can be enzymatically synthesized from amylopectin. The branching structure is similar to but more regular than natural glycogens (Kajiura, Takata, Kuriki, & Kitamura, 2010; Takata, Kajiura, Furuyashiki, Kakutani, & Kuriki, 2009). Since the obtained material has molar mass around 200 – 300 kg mol^{-1} and high solubility in water, HBCD, for which branching structure is schematically shown in Fig. 1(a), has been launched as a water-soluble carbohydrate source with low osmotic pressure (Takii et al., 2005). The sphere-like structure was confirmed for the similarly prepared glucan dendrimers by means of the small-angle X-ray scattering (Kageyama, Yanase, & Yuguchi, 2019). Anionic charged (Takemoto et al., 2013) and amphiphilic (Takeda et al., 2019) derivatives were thus synthesized to develop various applications. The commercially available HBCD sample as a reagent is, therefore, a good source of the hyperbranched polymers.

It is well known that fully substituted amylose carbamate derivatives have high chain stiffness and high solubility in organic solvents (Burchard, 1965, 2008; Pfannemuller, Schmidt, Ziegast, & Matsuo, 1984; Terao & Sato, 2018) whereas amylose behaves as relatively flexible chains (Jiang, Kitamura, Sato, & Terao, 2017; Nakanishi, Norisuye, Teramoto, & Kitamura, 1993) except for a specific solvent system (Seger, Aberle, & Burchard, 1996). Especially, amylose tris(3,5-dimethylphenylcarbamate) (ADMPC) has very high Kuhn segment length L_K of 73 nm, a measure of the chain stiffness, in 4-methyl-2-pentanone (MIBK) while it behaves as semiflexible chain with L_K = 23 nm in methyl acetate (MEA) (Tsuda et al., 2010). Furthermore, taking into account that amylose [α-(1-4) glucan] and starch tend to aggregate in aqueous media, 3,5-dimethylphenylcarbamate derivative of HBCD can be a good model highly branched (or hyperbranched) polymer consisting of rigid and semiflexible subchains. In this study, we thus synthesized HBCD tris(3,5-dimethylphenylcarbamate) (HDMPC, Fig. 1) from the commercially available HBCD sample. Conformational properties in the two solvents were studied from the dimensional and hydrodynamic properties in terms of the known theory for hyperbranched polymers (Lederer & Burchard, 2015).

ADMPC is one of the most utilized chiral selectors for the chiral (or enantioselective) HPLC (Shen & Okamoto, 2016). The chiral separation ability for amylopectin phenylcarbamate derivatives was somewhat different from those for the linear amylose based chiral selector (Félix & Zhang, 1993a, 1993b; P. Wang, Liu, Jiang, Gu, & Zhou, 2007). Furthermore, we recently found that chiral columns made of cyclic ADMPC (cADMPC) has also different chiral separation ability from that of the linear ADMPC (Ryoki, Kimura,

Kitamura, Maeda, & Terao, 2019). We thus studied chiral separation ability of a chiral column made of the HDMPC sample.

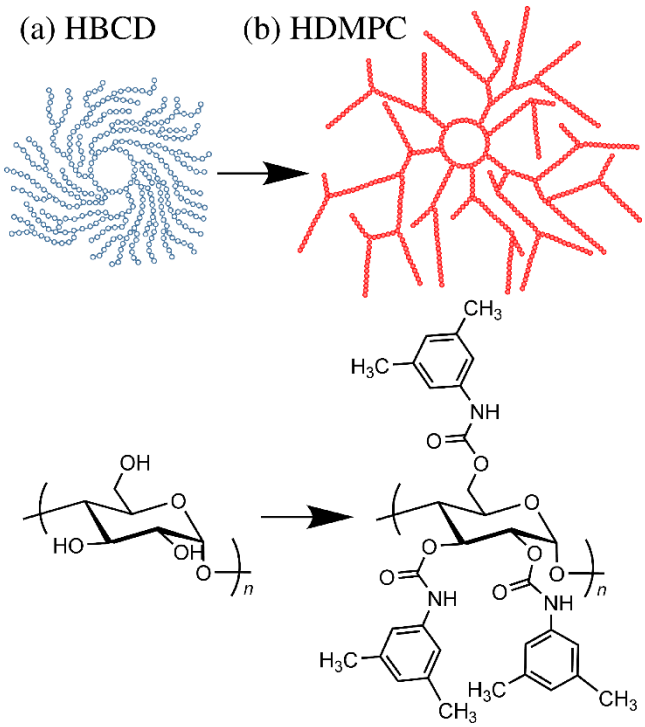

Fig. 1. Schematic representation of the branching structure and chemical structure of (a) HBCD and (b) HDMPC.

Experimental Section

HDMPC Sample. A reagent grade HBCD sample was purchased from Fujifilm-Wako produced by Ezaki Glico Co. The branching structure of the HBCD sample is substantially the same as but the residual oligosaccharides are fewer than those for the food grade, Cluster Dextrin™. The synthesis method of HDMPC was essentially the same as those for linear and cyclic ADMPC (cADMPC) samples (Ryoki et al., 2017; Tsuda et al., 2010). The procedure is described as follows. The HBCD sample (2.72 g, 16.8 mmol as the glucose unit) with lithium chloride (2.89 g, Fujifilm) were dried in a vacuum at 95 °C for 24 h in a round-bottom glass flask. *N*,*N*-dimethylacetamide (40 mL, Fujifilm, dehydrated grade) was added and stirred for 24 h at 90 °C to dissolve completely the HBCD sample. After pyridine (90 mL) was poured into the mixture, 3,5-dimethylphenyl isocyanate (25.3 g, 172 mmol, Fujifilm) was added, and then the mixture was stirred at 100 °C for 3 h. Guaranteed reagent grade of pyridine (Fujifilm) was distilled over calcium hydride prior to use. The resulting mixture cooled to room temperature was poured into methanol (2.5 L) to precipitate HDMPC. White precipitate was separated by centrifugation with 7000 G for 30 min. The crude sample was dried in a vacuum and dissolved in MEA. The insoluble part was removed by centrifugation and filtration. The soluble part was reprecipitated into methanol. It is known that the residual isocyanate and the low molar mass reactant were removed in this procedure (Ryoki et al., 2017). The obtained sample was designated as **HDMPC847k** based on the molar mass described below.

^{1}H NMR measurement was made for **HDMPC847k** in $CDCl_3$ with a JEOL ECS-400 spectrometer. The resulting NMR spectrum in Fig. S1 in the Supporting Information is consistent with the chemical structure of HDMPC while the signal for the hydrogen atoms on the pyranose ring was very weak because of the low mobility. The weight ratio of nitrogen to oxygen was determined from the ultimate analysis to be 0.109, which is quite close to the full substitution value of 0.106. The obtained sample can be dissolved in MEA, MIBK, and

tetrahydrofuran (THF) whereas linear ADMPC is not soluble in THF at room temperature, showing linear contaminant is negligible.

Size-exclusion chromatography (SEC). The weight-average molar mass M_w and the dispersity index $Đ$, the ratio of M_w to the number-average molar mass, were determined by SEC equipped with a DAWN DSP multi-angle light scattering (MALS) photometer (Wyatt) and a refractive index detector (Jasco). THF was chosen for the eluent. A TSKguardcolumn HXL-H and a TSKgel GMH$_{XL}$ column (Tosoh) were connected in series. The flow rate and the volume of the sample loop were 0.5 mL min^{-1} and 100 μL, respectively. The polymer mass concentration c was adjusted as 3.84 mg mL^{-1}. The detectors were calibrated with a standard polystyrene sample (Tosoh, TSKgel Standard F-4, M_w = 37.9 kg mol^{-1}). The refractive index increment was assumed to be the same as that for cADMPC in THF (0.165 cm^{3}g^{-1}) (Ryoki et al., 2017). A monomodal peak was obtained for the sample as shown in Fig. S2 in the supporting information. The evaluated M_w and $Đ$ values from the chromatogram are 847 kg mol^{-1} and 1.29, respectively. Since the molar mass M_0 of the repeat unit is 0.6037 kg mol^{-1}, the weight-average degree of polymerization N_w is calculated to be 1400.

Small-angle X-ray Scattering (SAXS). The form factor $P(q)$ and the radius of gyration R_g of **HDMPC847k** in MEA and MIBK at 25 °C were determined from SAXS measurements performed at the BL40B2 beamline in SPring-8 (Hyogo, Japan). The wavelength of the incident X-ray, the sample-to-detector distance (camera length), and accumulation time were chosen as 0.10 nm, 4.2 m, and 180 s, respectively. A quartz capillary with the diameter of 2.0 mmϕ was fixed in an aluminum block. This capillary cell was used both for the solutions and solvents. The position of the direct beam and the camera length on a Dectris Pilatus3 S 2M silicon pixel detector was determined by using the diffraction of silver behenate. Angular dependence of the scattering intensity $I(q)$ with q being the magnitude of the scattering vector were calculated from the two-dimensional image with the SAngler circular averaging software (N. Shimizu et al., 2016). To compensate the intensity fluctuation of the incident light and the transparency of the cell including the solution, the evaluated $I(q)$ data were calibrated by the intensity of the incident light detected at the lower end of the capillary. Solvent and solutions with four different c ranging between 4 and 20 mg mL^{-1} were measured in the same capillary to determine the excess scattering intensity $\Delta I(q)$. The resulting c dependence of $\Delta I(q)/c$ was appreciable only in the lowest q region (Fig. S3). This is typical for polymer-good solvent systems. The Guinier plot was utilized to analyze the extrapolated values $[\Delta I(q)/c]_{c\to 0}$ to infinite dilution (Fig. S4). The R_g value was obtained from the initial slope. We also measured the original HBCD sample in aqueous media, but the data were not further analyzed due to significant aggregates.

Viscometry. Solvent and solution viscosities of **HDMPC847k** in MEA and MIBK at 25 °C were measured with a conventional Ubbelohde viscometer for which the share rate is in the order of 1000 s^{-1}. The relative viscosity ranging between 1.15 and 1.7 were evaluated by taking the difference between the solution and solvent densities into account. The Huggins constant k' was obtained to be 1.3 and 0.94 for **HDMPC847k** in MEA and MIBK, respectively. Similar high k' was found for the other multibranched polymers (Hokajo, Terao, Nakamura, & Norisuye, 2001; Terao, Hokajo, Nakamura, & Norisuye, 1999).

Preparation of Chiral Column. A coated-type chiral stationary phase (CSP) was prepared from **HDMPC847k** as in the case with our recent research for ADMPC and cADMPC (Ryoki et al., 2019). This method is substantially the same as that for Okamoto et al. (Okamoto, Aburatani, Fukumoto, & Hatada, 1987). 3-Aminopropyltriethoxysilane treated silica gel (A-

silica) was prepared from a wide-pore silica gel (Daiso gel SP-1000-7, Osaka Soda) in the manner reported previously (Shen, Ikai, & Okamoto, 2010; I. Shimizu, Yoshino, Okabayashi, Nishio, & O'Connor, 1997). A THF solution (4.22 mL) of **HDMPC847k** (232 mg) was added dropwise to the A-silica sample (898 mg) and the solvent was evaporated in an eggplant flask. The obtained CSP was dried in a vacuum for 3 days. The resulting CSP was packed in a stainless-steel column (Chemco Plus, Osaka, Japan) with 2.1 mm of the inner diameter and 250 mm of the length by using a slurry method. The CSP (0.8571 g) was dispersed in 2-propanol (30 mL) by means of ultrasonication. The obtained suspension was filtered with a stainless-steel mesh (270 mesh) and incubated at room temperature for 1 h to precipitate the CSP. The precipitant was dispersed in 2-propanol (30 mL) again and filled into the column with a specially designed column packer and a DP-8020 HPLC pump (Tosoh, Tokyo, Japan). The flow rate was set to be 1.4 mL min^{-1} to achieve the back pressure of 30 – 40 MPa for about 4 h.

Chiral HPLC Test. Chiral separation performance of the **HDMPC847k** column and a previously reported **ADMPC49k** column (Ryoki et al., 2019) were tested with the following racemates: **1.** flavanone (TCI), **2.** 6,6'-dibromo-1,1'-bi-2-naphthol (TCI), **3.** trans-stilbene oxide (Sigma-Aldrich), **4.** Tröger's base (Fujifilm), **5.** 1,1'-bi-2-naphthol (TCI), **6.** benzoin (Fujifilm), **7.** anisoin (TCI), **8.** α-benzoin oxime (Alfa Aesar), **9.** 2,2,2-trifluoro-1-(9-anthryl)ethanol (Fujifilm), **10.** 4-methylbenzhydrol (TCI), **11.** 1-(2-Naphthyl)ethanol (TCI), **12.** tropic acid (Combi-Blocks), **13.** 2-(4-chlorophenyl)-3-methylbutyric acid (Combi-Blocks), **14.** 3-hydroxy-3-phenylpropionic acid (TCI). Their chemical structures are summarized in Fig. 2. Each column was installed into an HPLC system equipped with a Chromaster 5160 pump (Hitachi, Tokyo, Japan), a Rheodyne 7125 injector with a 20 μL sample loop, an online UV absorption detector (UV-8001, Tosoh) with the wavelength λ_0 = 254 nm in a vacuum, and an SF-3120 fraction collector (Advantec, Tokyo, Japan). The mobile phase and the flow rate were chosen to be hexane/2-propanol (9/1) and 0.1 mL min^{-1}, respectively. The plate number N and the dead volume V_0 of the column were estimated from the peak shape of benzene (Fujifilm) and 1,3,5-tri-tert-butylbenzene (TCI), respectively. The N value was evaluated to be 1984 for the column. When we observed two peaks in the chromatogram, circular dichroism (CD) measurements were made on a J-720WO CD spectrometer (Jasco, Tokyo, Japan) to characterize each fraction (Fig. S5). One of the fractions having negative CD signal at the highest λ_0 was designated to be (–) and the other was named as (+); noted that the sign of the CD signal at the highest λ_0 was not recognizable for some racemates. Retention volumes were determined as the peak-top positions for each chromatogram to estimate capacity factors k_1 and k_2 with $k_1 < k_2$, where k_x (x = 1 or 2) is defined with the peak retention volume V_x as

$$k_x = \frac{V_x - V_0}{V_0} \quad (1)$$

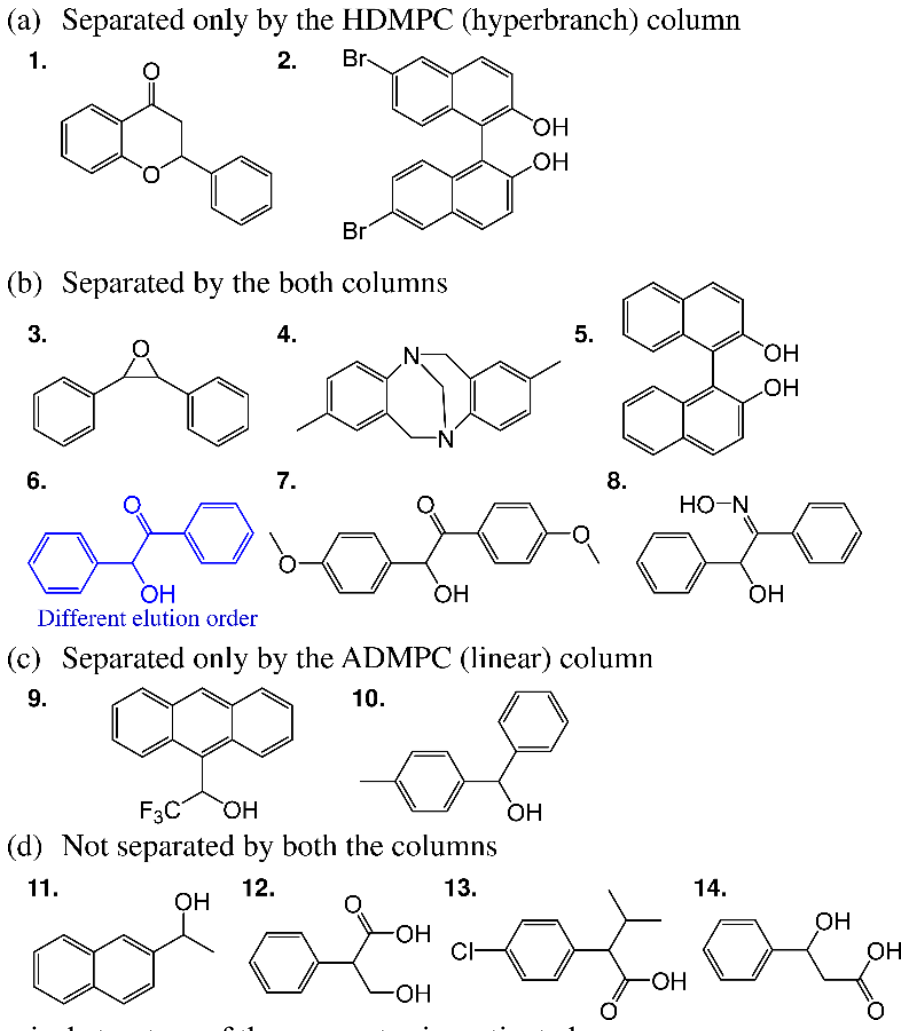

Fig. 2. Chemical structure of the racemates investigated.

Results and Discussion

Dimensional and Hydrodynamic Properties in Dilute Solution. Chain dimensions of branched polymers are generally much smaller than that for the corresponding linear chains with the same molar mass. The radius of gyration R_g data for HDMPC in the two solvents are plotted against M_w in Fig. 3(a) along with the literature values for linear ADMPC (Tsuda et al., 2010). While the maximum M_w for linear ADMPC is 340 kg mol^{-1}, we extrapolated it with the Benoit-Doty equation (Benoit & Doty, 1953) for the wormlike chain with the parameters in ref (Tsuda et al., 2010) to estimate the radius of gyration $R_{g,lin}$ value for the linear ADMPC with M_w = 847 kg mol^{-1} as 45 and 73 nm in MEA and MIBK, respectively. Then, the radius of gyration contraction factor g_s defined as $R_{g,br}^2$ / $R_{g,lin}^2$ is calculated to be 0.109 and 0.047 in the two solvents, respectively, with $R_{g,br}$ being R_g for the branched chain. The lower g_s value in MIBK than that in MEA is attributed to the hyperbranched polymer consisting of rodlike subchains. On the other hand, solvent dependency of R_g for **HDMPC847k** is much weaker than that for linear ADMPC with the same M_w. This is most likely due to relatively short subchains and high flexibility at the branching point. Indeed, considering that the α-1,6-linkage hydrolyzed HBCD sample has degree of polymerization of 16, the contour length L of the ADMPC subchain is 5.9 nm, and hence, the end-to-end distance can be estimated as 5.47 and 5.75 nm in MEA and MIBK, respectively. The ratio of the distances (5.47 / 5.75 = 0.951) in the two solvents is similar to that for the R_g values (Table 1, 0.949), thus reasonable.

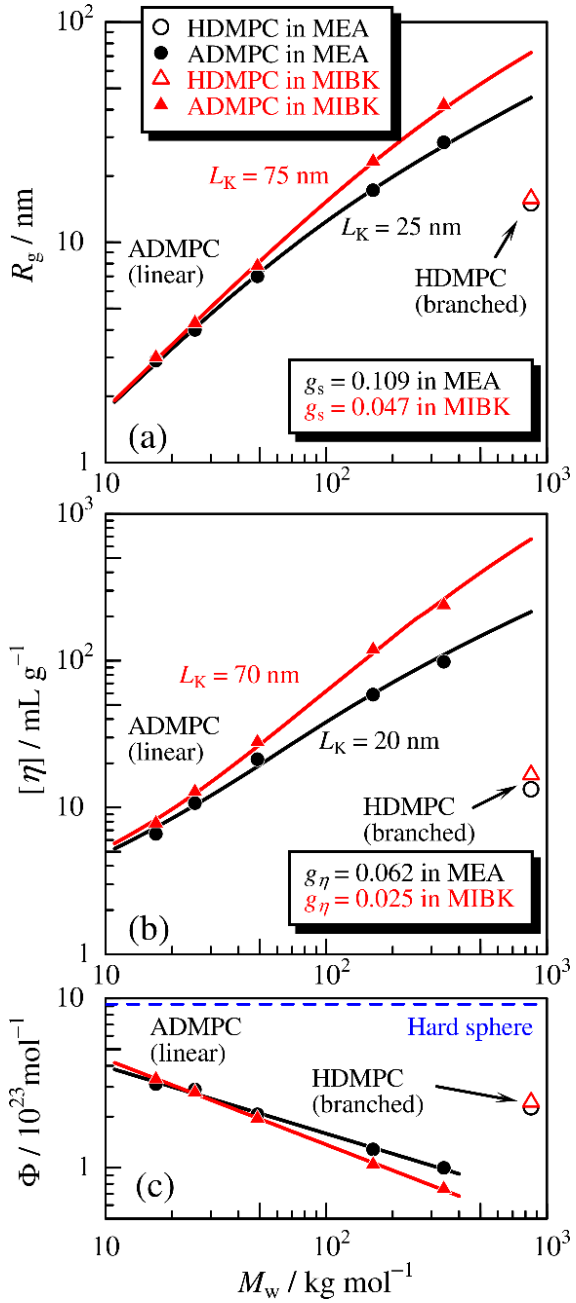

Fig. 3. M_w dependence of (a) R_g, (b) $[\eta]$, and (c) Φ for **HDMPC847K** (unfilled symbols) and ADMPC (Tsuda et al., 2010) in MEA (circles) and in MIBK (triangles) both at 25 °C. The solid black and red curves in panels (a) and (b) denote theoretical values of the wormlike chain for linear ADMPC in MEA and MIBK (Tsuda et al., 2010), respectively.

Table 1
Molecular parameters of **HDMPC847k**

Solvent	L_K / nm ***a***	R_g / nm	g_s	$[\eta]$ / mL g^{-1}	g_η	Φ / 10^{23}mol^{-1}	***d b***	$R_{g,HB}$ / nm ***b***
MEA	23	15.0	0.109	13.3	0.062	2.27	1.83	16.1
MIBK	73	15.8	0.047	16.7	0.025	2.44	1.75	17.5

a: For linear ADMPC. ***b***: Model Parameters for eq 4.

The branching effects can be recognized more significantly in $[\eta]$ as shown in Fig. 3(b) for which $[\eta]$ for **HDMPC847k** were determined to be 13.3 and 16.7 mL g^{-1} in MEA and

MIBK, respectively. Somewhat larger $[\eta]$ value in MIBK is attributed to the higher chain stiffness. Indeed, the intrinsic viscosity shrink factor g_η defined as $[\eta]_{br}$ / $[\eta]_{lin}$ are calculated to be 0.062 and 0.025 in the two solvents when the intrinsic viscosity $[\eta]_{lin}$ for the corresponding linear chain with the same M_w is estimated to be 215 and 673 mL g^{-1} in terms of the Yoshizaki-Nitta-Yamakawa theory (Yamakawa & Yoshizaki, 2016; Yoshizaki, Nitta, & Yamakawa, 1988) for the touched-bead wormlike chain with the parameters for linear ADMPC reported in ref (Tsuda et al., 2010).

The Flory viscosity factor Φ defined by

$$\Phi \equiv \frac{[\eta]M}{6^{3/2}{R_g}^3} \tag{2}$$

is plotted against M_w in Fig. 3(c) with those for the linear ADMPC. The obtained values listed in Table 1 are intermediate between the hard sphere (9.23×10^{23} mol^{-1}) and linear ADMPC ($< 1 \times 10^{23}$ mol^{-1}); incidentally close to the values for the linear flexible polymers (Yamakawa & Yoshizaki, 2016). Some hyperbranched polymers with flexible subchains have similar Φ value while it may depend on the branching degree (Lederer & Burchard, 2015; Lederer, Burchard, Khalyavina, Lindner, & Schweins, 2013). On the contrary, the ratio of hydrodynamic radius to R_g for glucan dendrimers in aqueous media was reported to be close to that for the rigid sphere (Kageyama et al., 2019; Takeda et al., 2019) despite the similar branching structure of HBCD. This difference is probably because of the high chain stiffness of HDMPC subchains.

The branching structure can influence the form factor $P(q)$ illustrated in Fig. 4. It is seen that the experimentally evaluated curve is much different from the linear chain (green dotted curve), for which the theoretical values were calculated by means of the touched bead wormlike chain (Burchard & Kajiwara, 1997; Nagasaka, Yoshizaki, Shimada, & Yamakawa, 1991; Yamakawa & Yoshizaki, 2016) with the known parameters (Tsuda et al., 2010). While the flat region is found at the lowest q range, steep reduction of $P(q)$ is found at the middle q region with the slope being −2.8 and −2.6 in MEA and MIBK, respectively. This is a specific behavior for hyperbranched polymers. Another interesting point is that the scattering intensity in the high q region is smaller than that for the linear chain even while substantially the same intensity was obtained for a star polymer with fewer arm numbers (Hasegawa, Nagata, Terao, & Suginome, 2017). This is probably because the large numbers of branching points as well as the dense segment density in the hyperbranched chains influence the scattering profile in the q range.

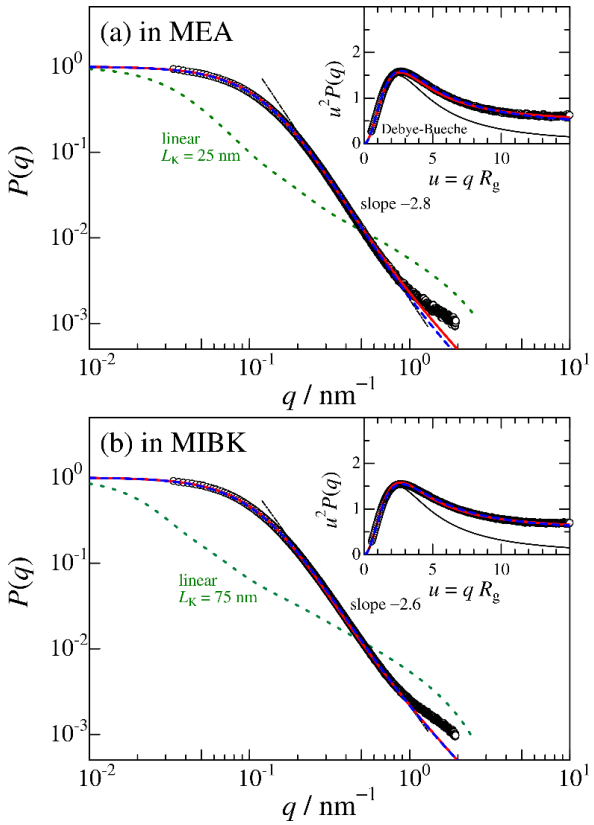

Fig. 4. Double logarithmic plots of the form factor $P(q)$ vs q for **HDMPC847K** (unfilled circles) in MEA (a) and in MIBK (b) both at 25 °C. The inset of each panel is the Kratky plot. Solid red and dashed blue curves denote the theoretical values from eq 3 (unperturbed) and eq 4 (perturbed) hyperbranched chains, respectively. Dotted green curves are the theoretical values of the wormlike chain for the linear ADMPC with the same M_w (Tsuda et al., 2010). Black solid curves in each inset are the Debye-Bueche scattering function.

According to Burchard et al. (Burchard, 1972, 2002; Lederer & Burchard, 2015), the form factor $P(u)$ for a Gaussian-chain based unperturbed hyperbranched chain model can be written as

$$P_0(u) = \frac{1+C_0\,u^2/3}{[1+(C_0+1)\,u^2/6]^2} \qquad (3)$$

where $1/C_0$ is the number of branching points per macromolecule of the number-average molar mass and $u = q\,R_{g,HB}$ with $R_{g,HB}$ being the gyration radii of the hyperbranched chain. If the HDMPC chains at the branching point is flexible and each subchain is not very long, this model can be applicable for HDMPC in solution. Indeed, when we choose $R_{g,HB}$ = 15.8 nm and $1/C_0$ = 24 in MEA and $R_{g,HB}$ = 17.0 nm and $1/C_0$ = 20 in MIBK, the theoretical red curves reproduce almost quantitatively the experimental data except for the high q region. The Kratky plot, the inset in each panel in Fig. 4, is broader than the Debye-Bueche equation, that is, $P_0(u)$ for $1/C_0 = \infty$, while glucan dendrimers in aqueous solution has sharper peak (Kageyama et al., 2019), behaving as rigid sphere. This difference is most likely because much higher chain stiffness of the ADMPC subchains of HDMPC than that for HBCD.

According to Takata et al. (Takata et al., 2003; Takata et al., 1996), α-1,6-linkage hydrolyzed HBCD sample by isoamylase has number-average degree of polymerization of 16. Consequently, number of branching point per molecule is roughly estimated to be 70. The evaluated $1/C_0$ values (20 or 24) are much smaller than this value. Taking the intramolecular

excluded volume effects into account, Burchard (Burchard, 2004) also proposed the form factor $P(u)$ for the perturbed hyperbranched chain to explain the form factor in good solvent systems by means of the fractal approach. The resulting expression is as follows.

$$P(u) = \left[\frac{\sin[(d-1)\arctan(\zeta_{\mathrm{br}}u)]}{(d-1)(\zeta_{\mathrm{br}}u)\left(1+{\zeta_{\mathrm{br}}}^2u^2\right)^{(d-1)/2}}\right]^2 \Big/ \left[\frac{\sin[(d-1)\arctan(\zeta_{\mathrm{lin}}u)]}{(d-1)(\zeta_{\mathrm{lin}}u)\left(1+{\zeta_{\mathrm{lin}}}^2u^2\right)^{(d-1)/2}}\right] \quad (4)$$

with

$${\zeta_{\mathrm{br}}}^2 = \frac{C+1}{d(d+1)} \quad (5)$$

$${\zeta_{\mathrm{lin}}}^2 = \frac{2C}{d(d+1)} \quad (6)$$

where $1/C$ is the number of branching points and d is the fractal dimension of the linear chain; note that $d = 2.0$ and $d = 1.7$ correspond to the unperturbed and perturbed chains, respectively (Burchard, 2004). Assuming $1/C = 70$, a curve fitting procedure was examined to estimate d and $R_{\mathrm{g,HB}}$. The discrepancy between theoretical values and experimental data becomes appreciable in the range of $q > 1$ nm^{-1}. This is probably due to the local structure of HDMPC. Indeed, the difference is substantially the same as the scattering intensity from the repeat unit of ADMPC, that is, $P(u) + 1/N_{\mathrm{w}}$ well explains the experimental $P(q)$ data (not shown here). This is similar behavior with the small-angle neutron scattering data for hyperbranched aliphatic-aromatic polyesters (Burchard et al., 2012). The good agreement between the experimental data and the theoretical values may be due to not straight conformation of HDMPC at each branching point. The d values were evaluated to be 1.83 and 1.75 in MEA and MIBK, respectively while R_{g} values were 16.1 and 17.5 nm. The former parameters are somewhat larger than 1.7, suggesting the solvent quality is between good and theta solvents. As a result, the larger d value in MEA than that in MIBK is consistent with the lower second virial coefficient for linear ADMPC reported previously (Tsuda et al., 2010). It should be noted that the R_{g} values are 7 – 11 % larger than those from the Guinier plot, suggesting that the current Guinier analysis slightly underestimate the R_{g} value. We may thus conclude that this model can reasonably explain the conformational feature of hyperbranched chain consisting of ADMPC subchains.

Chiral separation ability. To clarify whether complex polymer architecture of the HDMPC sample affects the molecular recognition ability of the chiral small molecules, we compared the chiral separation ability of **HDMPC847k** with those of linear and cyclic ADMPC (Ryoki et al., 2019) with the same mobile phase, *n*-hexane/2-propanol (9/1). Fig. 5 is some representative chromatograms for the **HDMPC847k** column and a previously reported ADMPC column (Ryoki et al., 2019). Bimodal peaks for the HDMPC column in panel (a) and ADMPC column for panel (b) correspond to two enantiomers. The elution volume was determined from the peak position of each peak to determine k_1 and k_2. The separation factor α defined as k_2/k_1 and the geometric average $\bar{k}$ of the capacity factor [$\equiv \sqrt{k_1 k_2}$] are plotted in Fig. 6. The latter $\bar{k}$ value significantly depends on the racemate, but similar value was observed for HDMPC, ADMPC, and cADMPC columns for which the preparation procedure is substantially the same each other (Ryoki et al., 2019), indicating the Gibbs energy of adsorption is not influenced by the chain architecture even though the high segment density of HDMPC molecules. Number of separatable racemates for the HDMPC column is the same as that for the ADMPC columns. Only the HDMPC column separates **1** and **2**, both the columns have enough resolution for **3** – **8**, and only the linear ADMPC column separates **9** and **10**.

Furthermore, the elution order of **6** is different between the two columns. This clearly shows that HDMPC column has high chiral separation ability and somewhat different separation behavior comparing with linear ADMPC even while separation ability can be somewhat influenced by the mobile phase. Fewer racemates can be separated by the cADMPC column, suggesting cyclic structure of HDMPC does not play an important role for the chiral separation ability. We may, therefore, conclude that many branching points and the high segment density of HDMPC molecules cause the difference in the separation ability between HDMPC and ADMPC columns. It should be noted that commercially available chiral columns made of linear ADMPC has significantly higher plate numbers as well as the baseline separation ability. We however chose our laboratory-made column for linear ADMPC because the effects on chain architecture should be compared for the chiral columns made by the same procedure.

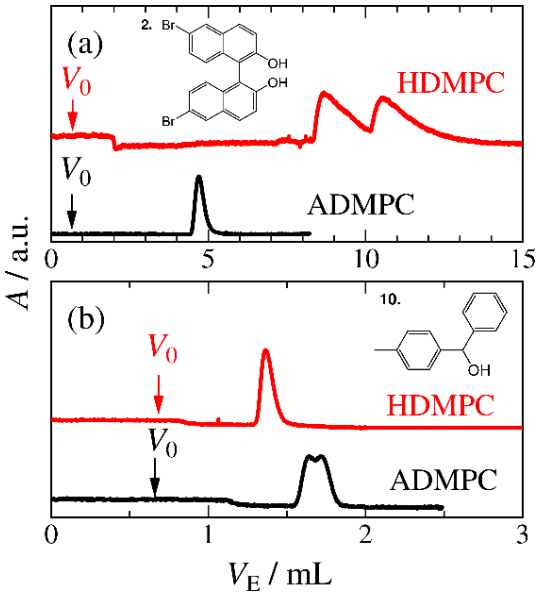

Fig. 5. Chromatograms of **2.** (A) and **10.** (B) on indicated CSPs with *n*-hexane/2-propanol (9/1) as the eluent. Arrows indicate the dead volume (V_0) of the column.

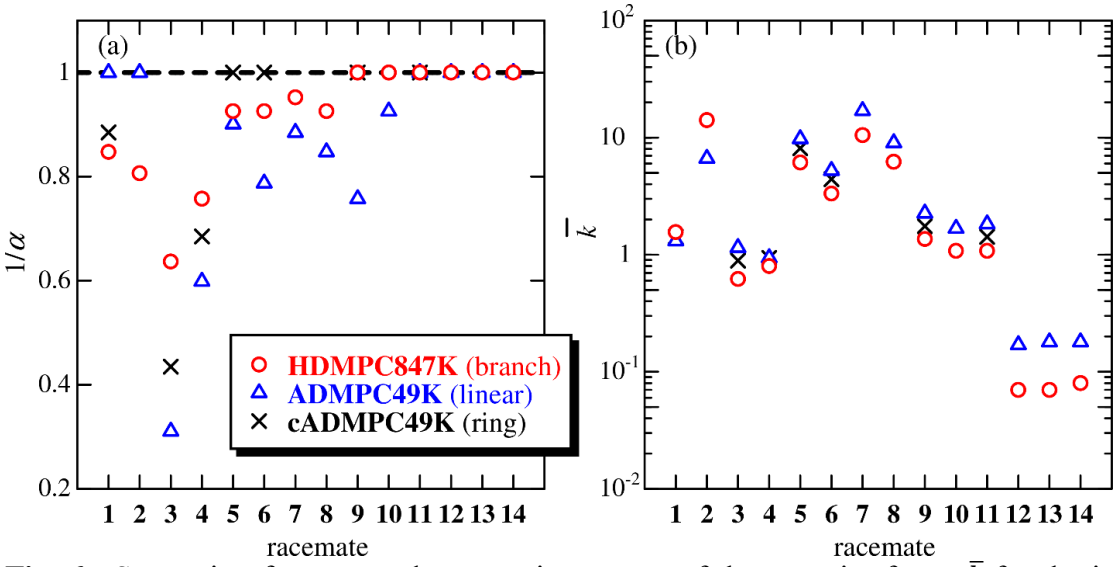

Fig. 6. Separation factor α and geometric average of the capacity factor $\bar{k}$ for the indicated CSPs with *n*-hexane/2-propanol (9/1) as the eluent. Chemical structures of each racemates are shown in Fig. 2.

Conclusions

We successfully synthesized a hyperbranched polysaccharide derivative (HDMPC) for which the main chain behaves as stiff chain with the Kuhn segment length of 23 and 73 nm in MEA and MIBK, respectively. Both the gyration contraction factor g_s and the viscosity contraction factor g_η in MIBK were evaluated to be 0.047 and 0.025. These very small values are the characteristics of the dimensional and hydrodynamic properties for hyperbranched polymers consisting of rigid subchains. Unlike recently investigated hyperbranched polysaccharide (glucan dendrimers) in aqueous media (Kageyama et al., 2019; Takeda et al., 2019), the Flory viscosity factor Φ determined from R_g and $[\eta]$ are close to that for the random coil. This is consistent with the previously investigated flexible hyperbranched polymers (Lederer & Burchard, 2015). The form factor $P(q)$ can also be explained by the known theories for the hyperbranched polymers with reasonable branching number. The chiral stationary phase made of the HDMPC sample shows chiral recognition ability with the mobile phase composed of *n*-hexane/1-propanol. Taking the commercial availability of this hyperbranched polysaccharide into account, it can be a good hyperbranched model polymer with stiff subchains.

Supporting Information

Additional figures for ^{1}H-NMR, SEC-MALS, SAXS, CD, and chiral HPLC data.

Acknowledgments

The authors are grateful to Prof. Takahiro Sato (Osaka Univ.) for fruitful discussion and to Dr. Noboru Ohta (SPring-8) for SAXS measurements. The synchrotron radiation experiments were performed at the BL40B2 in SPring-8 with the approval of the Japan Synchrotron Radiation Research Institute (JASRI) (proposal No. 2020A1132). The NMR measurement and ultimate analysis were performed at the Analytical Instrument Facility, Graduate School of Science, Osaka University. This work was partly supported by JSPS KAKENHI grant numbers JP17K05884 and JP20H02788.

References

Benoit, H., & Doty, P. (1953). Light Scattering from Non-Gaussian Chains. *The Journal of Physical Chemistry,* 57(9), 958-963.

Bonaccorsi, L., Calandra, P., Amenitsch, H., Proverbio, E., & Lombardo, D. (2013). Growth of fractal aggregates during template directed SAPO-34 zeolite formation. *Microporous and Mesoporous Materials,* 167, 3-9.

Burchard, W. (1965). Uber Die Abweichungen Von Der Idealen Knauelstatistik Bei Amylose- Und Cellulosetricarbanilat in Einem Theta-Losungsmittel. *Makromolekulare Chemie,* 88(Oct), 11-&.

Burchard, W. (1972). Angular-Distribution of Rayleigh-Scattering from Branched Polycondensates - Amylopectin and Glycogen Types. *Macromolecules,* 5(5), 604-&.

Burchard, W. (2002). Particle Scattering Factors of Some Branched Polymers. *Macromolecules,* 10(5), 919-927.

Burchard, W. (2004). Angular dependence of scattered light from hyperbranched structures in a good solvent. A fractal approach. *Macromolecules,* 37(10), 3841-3849.

Burchard, W. (2008). *Light Scattering from Polysaccharides as Soft Materials*. In R. Borsali & R. Pecora (Eds.), *Soft Matter Characterization* (pp. 463-603): Springer Netherlands

Burchard, W., & Kajiwara, K. (1997). The statistics of stiff chain molecules I. The particle scattering factor. *Proceedings of the Royal Society of London. A. Mathematical and Physical Sciences,* 316(1525), 185-199.

Burchard, W., Khalyavina, A., Lindner, P., Schweins, R., Friedel, P., Wiemann, M., & Lederer, A. (2012). SANS Investigation of Global and Segmental Structures of Hyperbranched Aliphatic-Aromatic Polyesters. *Macromolecules,* 45(7), 3177-3187.

Chen, H., & Kong, J. (2016). Hyperbranched polymers from A2 + B3 strategy: recent advances in description and control of fine topology. *Polymer Chemistry,* 7(22), 3643-3663.

Cook, A. B., & Perrier, S. (2020). Branched and Dendritic Polymer Architectures: Functional Nanomaterials for Therapeutic Delivery. *Advanced Functional Materials,* 30(2), 1901001.

Félix, G., & Zhang, T. (1993a). An amylopectin tris(phenylcarbamate) chiral stationary phase for high performance liquid chromatography. *Journal of High Resolution Chromatography,* 16(6), 364-367.

Félix, G., & Zhang, T. (1993b). Chiral packing materials for high-performance liquid chromatographic resolution of enantiomers based on substituted branched polysaccharides coated on silica gel. *Journal of Chromatography A,* 639(2), 141-149.

Hao, N., Zhu, M., & Li, L. (2019). Light Scattering Study of Internal Dynamics of Hyperbranched Polymers with Controlled Branching Patterns and Low Polydispersities in Dilute Solutions. *Macromolecules,* 52(10), 3794-3804.

Hasegawa, H., Nagata, Y., Terao, K., & Suginome, M. (2017). Synthesis and Solution Properties of a Rigid Helical Star Polymer: Three-Arm Star Poly(quinoxaline-2,3-diyl). *Macromolecules,* 50(19), 7491-7497.

Hirao, A., & Yoo, H.-S. (2011). Dendrimer-like star-branched polymers: novel structurally well-defined hyperbranched polymers. *Polymer Journal,* 43(1), 2-17.

Hokajo, T., Terao, K., Nakamura, Y., & Norisuye, T. (2001). Solution properties of polymacromonomers consisting of polystyrene - V. Effect of side chain length on chain stiffness. *Polymer Journal,* 33(6), 481-485.

Jiang, X. Y., Kitamura, S., Sato, T., & Terao, K. (2017). Chain Dimensions and Stiffness of Cellulosic and Amylosic Chains in an Ionic Liquid: Cellulose, Amylose, and an Amylose Carbamate in BmimCl. *Macromolecules,* 50(10), 3980-3985.

Kageyama, A., Yanase, M., & Yuguchi, Y. (2019). Structural characterization of enzymatically synthesized glucan dendrimers. *Carbohydrate Polymers,* 204, 104-110.

Kajiura, H., Takata, H., Kuriki, T., & Kitamura, S. (2010). Structure and solution properties of enzymatically synthesized glycogen. *Carbohydrate Research,* 345(6), 817-824.

Lederer, A., & Burchard, W. (2015). *Hyperbranched Polymers: Macromolecules in between Deterministic Linear Chains and Dendrimer Structures (Polymer Chemistry Series Vol. 16)*: Royal Society of Chemistry.

Lederer, A., Burchard, W., Khalyavina, A., Lindner, P., & Schweins, R. (2013). Is the universal law valid for branched polymers? *Angewandte Chemie. International Ed. In English,* 52(17), 4659-4663.

Nagasaka, K., Yoshizaki, T., Shimada, J., & Yamakawa, H. (1991). More on the scattering function of helical wormlike chains. *Macromolecules,* 24(4), 924-931.

Nakanishi, Y., Norisuye, T., Teramoto, A., & Kitamura, S. (1993). Conformation of Amylose in Dimethyl-Sulfoxide. *Macromolecules,* 26(16), 4220-4225.

Okamoto, Y., Aburatani, R., Fukumoto, T., & Hatada, K. (1987). Chromatographic Resolution .17. Useful Chiral Stationary Phases for Hplc - Amylose Tris(3,5-Dimethylphenylcarbamate) and Tris(3,5-Dichlorophenylcarbamate) Supported on Silica-Gel. *Chemistry Letters,* 16(9), 1857-1860.

Pfannemuller, B., Schmidt, M., Ziegast, G., & Matsuo, K. (1984). Properties of a Once-Broken Wormlike Chain Based on Amylose Tricarbanilate - Light-Scattering, Viscosity, and Dielectric-Relaxation. *Macromolecules,* 17(4), 710-716.

Ryoki, A., Kimura, Y., Kitamura, S., Maeda, K., & Terao, K. (2019). Does local chain conformation affect the chiral recognition ability of an amylose derivative? Comparison between linear and cyclic amylose tris(3,5-dimethylphenylcarbamate). *Journal of Chromatography A,* 1599, 144-151.

Ryoki, A., Yokobatake, H., Hasegawa, H., Takenaka, A., Ida, D., Kitamura, S., & Terao, K. (2017). Topology-Dependent Chain Stiffness and Local Helical Structure of Cyclic Amylose Tris(3,5-dimethylphenylcarbamate) in Solution. *Macromolecules,* 50(10), 4001-4007.

Seger, B., Aberle, T., & Burchard, W. (1996). Solution behaviour of cellulose and amylose in iron-sodiumtartrate (FeTNa). *Carbohydrate Polymers,* 31(1-2), 105-112.

Shen, J., Ikai, T., & Okamoto, Y. (2010). Synthesis and chiral recognition of novel amylose derivatives containing regioselectively benzoate and phenylcarbamate groups. *Journal of Chromatography A,* 1217(7), 1041-1047.

Shen, J., & Okamoto, Y. (2016). Efficient Separation of Enantiomers Using Stereoregular Chiral Polymers. *Chemical Reviews,* 116(3), 1094-1138.

Shimizu, I., Yoshino, A., Okabayashi, H., Nishio, E., & O'Connor, C. J. (1997). Kinetics of interaction of 3-aminopropyltriethoxysilane on a silica gel surface using elemental analysis and diffuse reflectance infrared Fourier transform spectra. *Journal of the Chemical Society, Faraday Transactions,* 93(10), 1971-1979.

Shimizu, N., Yatabe, K., Nagatani, Y., Saijyo, S., Kosuge, T., & Igarashi, N. (2016). Software Development for Analysis of Small-angle X-ray Scattering Data. *AIP Conference Proceedings,* 1741(1), 050017.

Takata, H., Kajiura, H., Furuyashiki, T., Kakutani, R., & Kuriki, T. (2009). Fine structural properties of natural and synthetic glycogens. *Carbohydrate Research,* 344(5), 654-659.

Takata, H., Ohdan, K., Takaha, T., Kuriki, T., & Okada, S. (2003). Properties of Branching Enzyme from Hyperthermophilic Bacterium, Aquifex aeolicus, and Its Potential for Production of Highly-branched Cyclic Dextrin. *Journal of Applied Glycoscience,* 50(1), 15-20.

Takata, H., Takaha, T., Okada, S., Hizukuri, S., Takagi, M., & Imanaka, T. (1996). Structure of the cyclic glucan produced from amylopectin by Bacillus stearothermophilus branching enzyme. *Carbohydrate Research,* 295, 91-101.

Takeda, S., Nishimura, T., Umezaki, K., Kubo, A., Yanase, M., Sawada, S.-I., . . . Akiyoshi, K. (2019). Synthesis and function of amphiphilic glucan dendrimers as nanocarriers for protein delivery. *Biomaterials Science,* 7(4), 1617-1622.

Takemoto, Y., Izawa, H., Umegatani, Y., Yamamoto, K., Kubo, A., Yanase, M., . . . Kadokawa, J. (2013). Synthesis of highly branched anionic alpha-glucans by thermostable phosphorylase-catalyzed alpha-glucuronylation. *Carbohydrate Research,* 366, 38-44.

Takii, H., Takii, Y., Kometani, T., Nishimura, T., Nakae, T., Kuriki, T., & Fushiki, T. (2005). Fluids Containing a Highly Branched Cyclic Dextrin Influence the Gastric Emptying Rate. *International Journal of Sports Medicine,* 26(4), 314-319.

Terao, K., Hokajo, T., Nakamura, Y., & Norisuye, T. (1999). Solution properties of polymacromonomers consisting of polystyrene. 3. Viscosity behavior in cyclohexane and toluene. *Macromolecules,* 32(11), 3690-3694.

Terao, K., & Sato, T. (2018). *Conformational Properties of Polysaccharide Derivatives*. In G. Yang & L. Lamboni (Eds.), *Bioinspired Materials Science and Engineering* (pp. 167-183)

Tsuda, M., Terao, K., Nakamura, Y., Kita, Y., Kitamura, S., & Sato, T. (2010). Solution Properties of Amylose Tris(3,5-dimethylphenylcarbamate) and Amylose Tris(phenylcarbamate): Side Group and Solvent Dependent Chain Stiffness in Methyl Acetate, 2-Butanone, and 4-Methyl-2-pentanone. *Macromolecules,* 43(13), 5779-5784.

Wang, D. L., Jin, Y., Zhu, X. Y., & Yan, D. Y. (2017). Synthesis and applications of stimuli-responsive hyperbranched polymers. *Progress in Polymer Science,* 64, 114-153.

Wang, P., Liu, D., Jiang, S., Gu, X., & Zhou, Z. (2007). The direct chiral separations of fungicide enantiomers on amylopectin based chiral stationary phase by HPLC. *Chirality,* 19(2), 114-119.

Yamago, S. (2021). Practical synthesis of dendritic hyperbranched polymers by reversible deactivation radical polymerization. *Polymer Journal,* 53(8), 847-864.

Yamakawa, H., & Yoshizaki, T. (2016). *Helical Wormlike Chains in Polymer Solutions, 2nd ed.* Berlin, Germany: Springer.

Yoshizaki, T., Nitta, I., & Yamakawa, H. (1988). Transport-Coefficients of Helical Wormlike Chains .4. Intrinsic-Viscosity of the Touched-Bead Model. *Macromolecules,* 21(1), 165-171.

Supplementary materials for

Molecular structure and chiral recognition ability of highly branched cyclic dextrin carbamate derivative

Aika Kishimoto,[a] Madoka Mizuguchi,[a] Akiyuki Ryoki,[a,b] and Ken Terao,[a,*]

[a]Department of Macromolecular Science, Graduate School of Science, Osaka University, 1-1 Machikaneyama-cho, Toyonaka, Osaka 560-0043, Japan.

[b]Department of Polymer Chemistry, Graduate School of Engineering, Kyoto University, Katsura, Kyoto 615-8510, Japan.

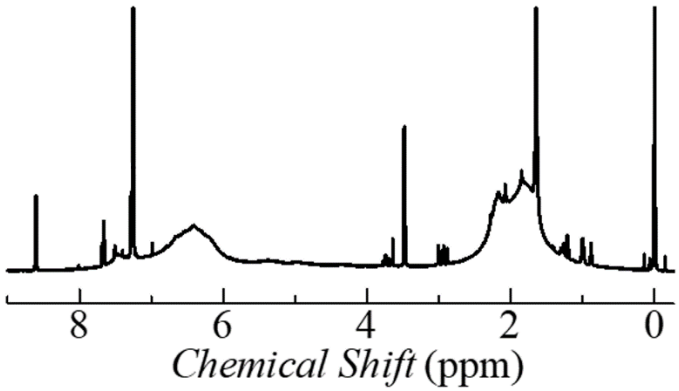

Fig. S1. ^{1}H NMR spectrum of **HDMPC847k** in $CDCl_3$ at 25˚C.

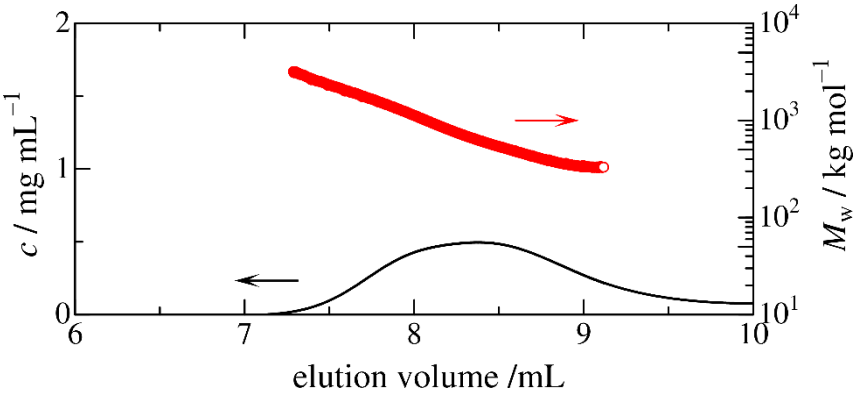

Fig. S2. Results from SEC-MALS measurement for **HDMPC847k** in THF at 25 °C.

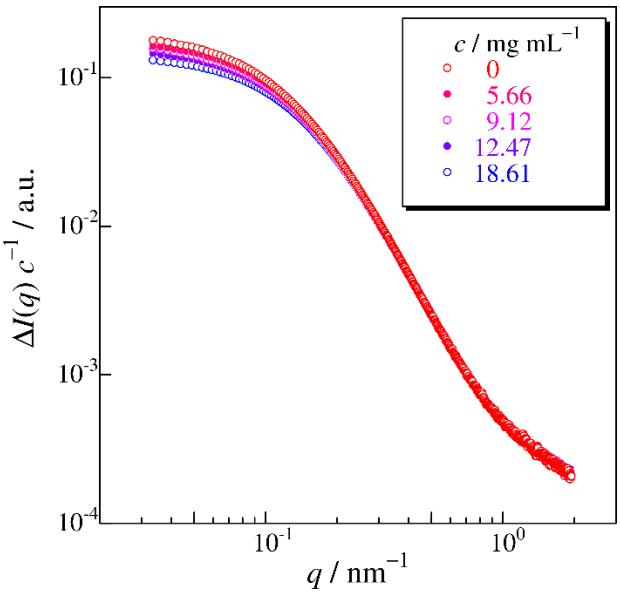

Fig. S3. q-dependence of the excess scattering intensity $\Delta I(q)$ divided by the polymer mass concentration c for **HDMPC847k** in methyl acetate (MEA) at indicated c at 25 °C.

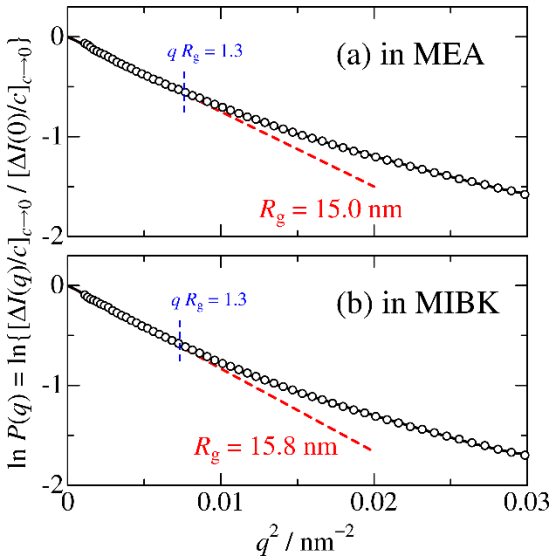

Fig. S4. Guinier plots for **HDMPC847k** in MEA (a) and in MIBK (b) both at 25 °C. Dashed red lines, initial slope to determine the radius of gyration R_g.

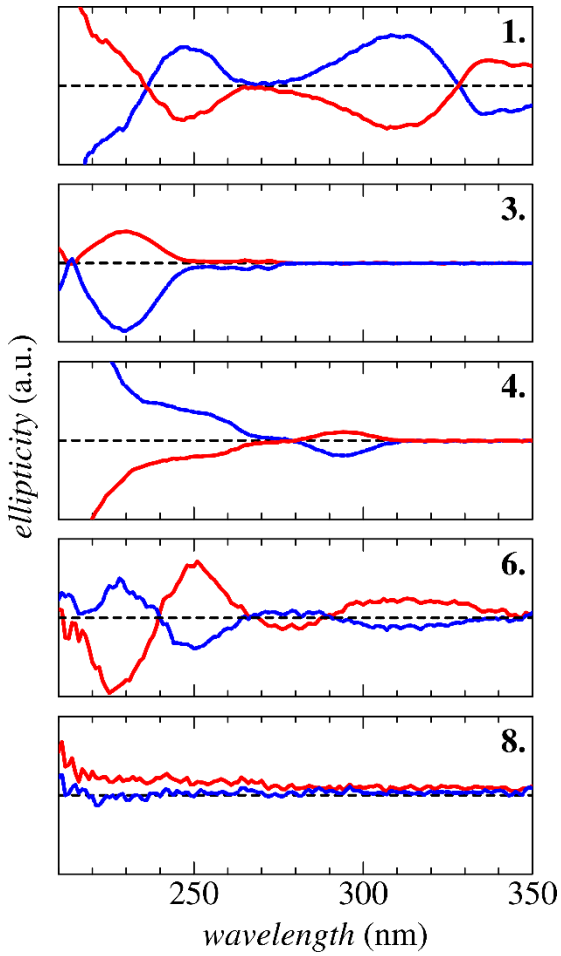

Fig. S5. CD spectra for the enantiomers separated from indicated racemates. Red and blue curves indicate spectra for (–) and (+), respectively, for each racemate.

Table S1

Geometric-average capacity factor $\bar{k}$ and separation factor α for the racemates (1-14) separated on **HDMPC847k**, **ADMPC49K**, and **cADMPC49K** columns with hexane/2-prapanaol (9/1) as the eluent

	HDMPC847k		**ADMPC49K**		**cADMPC49K**	
racemate	$\bar{k}$	α	$\bar{k}$	α	$\bar{k}$	α
1.	1.56	1.18 (−)	1.31 [a]	1 [a]	1.42 [a]	1.13 (−) [a]
2.	14.1	1.24	6.65	1		
3.	0.62	1.57 (+)	1.15 [a]	3.22 (+) [a]	0.89 [a]	2.3 (+) [a]
4.	0.8	1.32 (−)	0.94 [a]	1.67 (−) [a]	0.94 [a]	1.46 (−) [a]
5.	6.13	1.08	9.75 [a]	1.11 (−) [a]	8.11 [a]	1 [a]
6.	3.33	1.08 (+)	5.23 [a]	1.27 (−) [a]	4.42 [a]	1 [a]
7.	10.5	1.05	17.0	1.13		
8.	6.22	1.08 (+)	9.04	1.18		
9.	1.36	1	2.26 [a]	1.32 [a]	1.75 [a]	1 [a]
10.	1.08	1	1.68	1.08		
11.	1.08	1	1.83 [a]	1 [a]	1.42 [a]	1 [a]
12.	0.07	1	0.17	1		
13.	0.07	1	0.18	1		
14.	0.08	1	0.18	1		

a ref. (Ryoki et al., 2019). (+)(−) firstly eluted enantiomer.

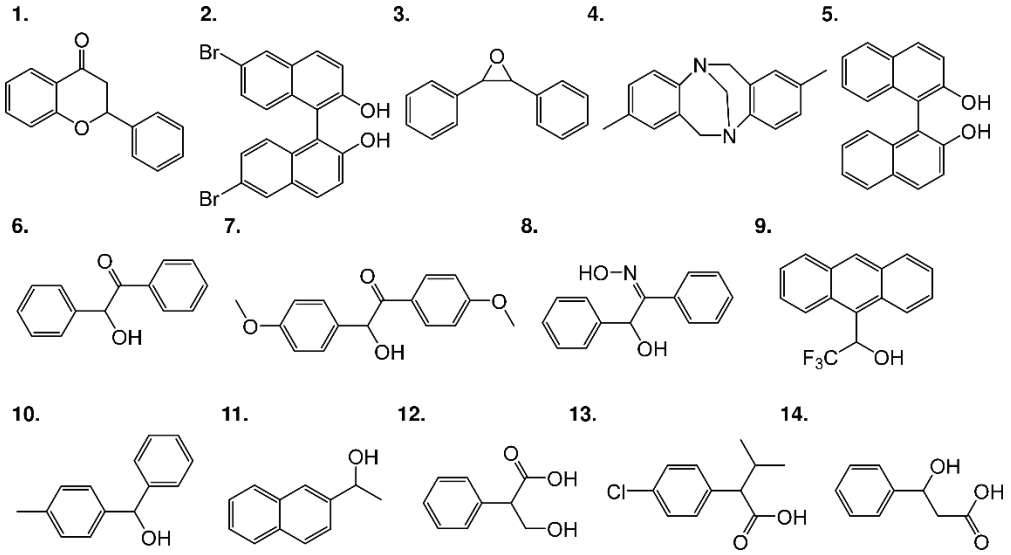

Reference

Benoit, H., & Doty, P. (1953). Light Scattering from Non-Gaussian Chains. *The Journal of Physical Chemistry,* 57(9), 958-963.

Bonaccorsi, L., Calandra, P., Amenitsch, H., Proverbio, E., & Lombardo, D. (2013). Growth of fractal aggregates during template directed SAPO-34 zeolite formation. *Microporous and Mesoporous Materials,* 167, 3-9.

Burchard, W. (1965). Uber Die Abweichungen Von Der Idealen Knauelstatistik Bei Amylose- Und Cellulosetricarbanilat in Einem Theta-Losungsmittel. *Makromolekulare Chemie,* 88(Oct), 11-&.
Burchard, W. (1972). Angular-Distribution of Rayleigh-Scattering from Branched Polycondensates - Amylopectin and Glycogen Types. *Macromolecules,* 5(5), 604-&.
Burchard, W. (2002). Particle Scattering Factors of Some Branched Polymers. *Macromolecules,* 10(5), 919-927.
Burchard, W. (2004). Angular dependence of scattered light from hyperbranched structures in a good solvent. A fractal approach. *Macromolecules,* 37(10), 3841-3849.
Burchard, W. (2008). *Light Scattering from Polysaccharides as Soft Materials*. In R. Borsali & R. Pecora (Eds.), *Soft Matter Characterization* (pp. 463-603): Springer Netherlands
Burchard, W., & Kajiwara, K. (1997). The statistics of stiff chain molecules I. The particle scattering factor. *Proceedings of the Royal Society of London. A. Mathematical and Physical Sciences,* 316(1525), 185-199.
Burchard, W., Khalyavina, A., Lindner, P., Schweins, R., Friedel, P., Wiemann, M., & Lederer, A. (2012). SANS Investigation of Global and Segmental Structures of Hyperbranched Aliphatic-Aromatic Polyesters. *Macromolecules,* 45(7), 3177-3187.
Chen, H., & Kong, J. (2016). Hyperbranched polymers from A2 + B3 strategy: recent advances in description and control of fine topology. *Polymer Chemistry,* 7(22), 3643-3663.
Cook, A. B., & Perrier, S. (2020). Branched and Dendritic Polymer Architectures: Functional Nanomaterials for Therapeutic Delivery. *Advanced Functional Materials,* 30(2), 1901001.
Félix, G., & Zhang, T. (1993a). An amylopectin tris(phenylcarbamate) chiral stationary phase for high performance liquid chromatography. *Journal of High Resolution Chromatography,* 16(6), 364-367.
Félix, G., & Zhang, T. (1993b). Chiral packing materials for high-performance liquid chromatographic resolution of enantiomers based on substituted branched polysaccharides coated on silica gel. *Journal of Chromatography A,* 639(2), 141-149.
Hao, N., Zhu, M., & Li, L. (2019). Light Scattering Study of Internal Dynamics of Hyperbranched Polymers with Controlled Branching Patterns and Low Polydispersities in Dilute Solutions. *Macromolecules,* 52(10), 3794-3804.
Hasegawa, H., Nagata, Y., Terao, K., & Suginome, M. (2017). Synthesis and Solution Properties of a Rigid Helical Star Polymer: Three-Arm Star Poly(quinoxaline-2,3-diyl). *Macromolecules,* 50(19), 7491-7497.
Hirao, A., & Yoo, H.-S. (2011). Dendrimer-like star-branched polymers: novel structurally well-defined hyperbranched polymers. *Polymer Journal,* 43(1), 2-17.
Hokajo, T., Terao, K., Nakamura, Y., & Norisuye, T. (2001). Solution properties of polymacromonomers consisting of polystyrene - V. Effect of side chain length on chain stiffness. *Polymer Journal,* 33(6), 481-485.
Jiang, X. Y., Kitamura, S., Sato, T., & Terao, K. (2017). Chain Dimensions and Stiffness of Cellulosic and Amylosic Chains in an Ionic Liquid: Cellulose, Amylose, and an Amylose Carbamate in BmimCl. *Macromolecules,* 50(10), 3980-3985.
Kageyama, A., Yanase, M., & Yuguchi, Y. (2019). Structural characterization of enzymatically synthesized glucan dendrimers. *Carbohydrate Polymers,* 204, 104-110.
Kajiura, H., Takata, H., Kuriki, T., & Kitamura, S. (2010). Structure and solution properties of enzymatically synthesized glycogen. *Carbohydrate Research,* 345(6), 817-824.
Lederer, A., & Burchard, W. (2015). *Hyperbranched Polymers: Macromolecules in between Deterministic Linear Chains and Dendrimer Structures (Polymer Chemistry Series Vol. 16)*: Royal Society of Chemistry.

Lederer, A., Burchard, W., Khalyavina, A., Lindner, P., & Schweins, R. (2013). Is the universal law valid for branched polymers? *Angewandte Chemie. International Ed. In English,* 52(17), 4659-4663.

Nagasaka, K., Yoshizaki, T., Shimada, J., & Yamakawa, H. (1991). More on the scattering function of helical wormlike chains. *Macromolecules,* 24(4), 924-931.

Nakanishi, Y., Norisuye, T., Teramoto, A., & Kitamura, S. (1993). Conformation of Amylose in Dimethyl-Sulfoxide. *Macromolecules,* 26(16), 4220-4225.

Okamoto, Y., Aburatani, R., Fukumoto, T., & Hatada, K. (1987). Chromatographic Resolution .17. Useful Chiral Stationary Phases for Hplc - Amylose Tris(3,5-Dimethylphenylcarbamate) and Tris(3,5-Dichlorophenylcarbamate) Supported on Silica-Gel. *Chemistry Letters,* 16(9), 1857-1860.

Pfannemuller, B., Schmidt, M., Ziegast, G., & Matsuo, K. (1984). Properties of a Once-Broken Wormlike Chain Based on Amylose Tricarbanilate - Light-Scattering, Viscosity, and Dielectric-Relaxation. *Macromolecules,* 17(4), 710-716.

Ryoki, A., Kimura, Y., Kitamura, S., Maeda, K., & Terao, K. (2019). Does local chain conformation affect the chiral recognition ability of an amylose derivative? Comparison between linear and cyclic amylose tris(3,5-dimethylphenylcarbamate). *Journal of Chromatography A,* 1599, 144-151.

Ryoki, A., Yokobatake, H., Hasegawa, H., Takenaka, A., Ida, D., Kitamura, S., & Terao, K. (2017). Topology-Dependent Chain Stiffness and Local Helical Structure of Cyclic Amylose Tris(3,5-dimethylphenylcarbamate) in Solution. *Macromolecules,* 50(10), 4001-4007.

Seger, B., Aberle, T., & Burchard, W. (1996). Solution behaviour of cellulose and amylose in iron-sodiumtartrate (FeTNa). *Carbohydrate Polymers,* 31(1-2), 105-112.

Shen, J., Ikai, T., & Okamoto, Y. (2010). Synthesis and chiral recognition of novel amylose derivatives containing regioselectively benzoate and phenylcarbamate groups. *Journal of Chromatography A,* 1217(7), 1041-1047.

Shen, J., & Okamoto, Y. (2016). Efficient Separation of Enantiomers Using Stereoregular Chiral Polymers. *Chemical Reviews,* 116(3), 1094-1138.

Shimizu, I., Yoshino, A., Okabayashi, H., Nishio, E., & O'Connor, C. J. (1997). Kinetics of interaction of 3-aminopropyltriethoxysilane on a silica gel surface using elemental analysis and diffuse reflectance infrared Fourier transform spectra. *Journal of the Chemical Society, Faraday Transactions,* 93(10), 1971-1979.

Shimizu, N., Yatabe, K., Nagatani, Y., Saijyo, S., Kosuge, T., & Igarashi, N. (2016). Software Development for Analysis of Small-angle X-ray Scattering Data. *AIP Conference Proceedings,* 1741(1), 050017.

Takata, H., Kajiura, H., Furuyashiki, T., Kakutani, R., & Kuriki, T. (2009). Fine structural properties of natural and synthetic glycogens. *Carbohydrate Research,* 344(5), 654-659.

Takata, H., Ohdan, K., Takaha, T., Kuriki, T., & Okada, S. (2003). Properties of Branching Enzyme from Hyperthermophilic Bacterium, Aquifex aeolicus, and Its Potential for Production of Highly-branched Cyclic Dextrin. *Journal of Applied Glycoscience,* 50(1), 15-20.

Takata, H., Takaha, T., Okada, S., Hizukuri, S., Takagi, M., & Imanaka, T. (1996). Structure of the cyclic glucan produced from amylopectin by Bacillus stearothermophilus branching enzyme. *Carbohydrate Research,* 295, 91-101.

Takeda, S., Nishimura, T., Umezaki, K., Kubo, A., Yanase, M., Sawada, S.-I., . . . Akiyoshi, K. (2019). Synthesis and function of amphiphilic glucan dendrimers as nanocarriers for protein delivery. *Biomaterials Science,* 7(4), 1617-1622.

Takemoto, Y., Izawa, H., Umegatani, Y., Yamamoto, K., Kubo, A., Yanase, M., . . . Kadokawa, J. (2013). Synthesis of highly branched anionic alpha-glucans by thermostable phosphorylase-catalyzed alpha-glucuronylation. *Carbohydrate Research,* 366, 38-44.

Takii, H., Takii, Y., Kometani, T., Nishimura, T., Nakae, T., Kuriki, T., & Fushiki, T. (2005). Fluids Containing a Highly Branched Cyclic Dextrin Influence the Gastric Emptying Rate. *International Journal of Sports Medicine,* 26(4), 314-319.

Terao, K., Hokajo, T., Nakamura, Y., & Norisuye, T. (1999). Solution properties of polymacromonomers consisting of polystyrene. 3. Viscosity behavior in cyclohexane and toluene. *Macromolecules,* 32(11), 3690-3694.

Terao, K., & Sato, T. (2018). *Conformational Properties of Polysaccharide Derivatives*. In G. Yang & L. Lamboni (Eds.), *Bioinspired Materials Science and Engineering* (pp. 167-183)

Tsuda, M., Terao, K., Nakamura, Y., Kita, Y., Kitamura, S., & Sato, T. (2010). Solution Properties of Amylose Tris(3,5-dimethylphenylcarbamate) and Amylose Tris(phenylcarbamate): Side Group and Solvent Dependent Chain Stiffness in Methyl Acetate, 2-Butanone, and 4-Methyl-2-pentanone. *Macromolecules,* 43(13), 5779-5784.

Wang, D. L., Jin, Y., Zhu, X. Y., & Yan, D. Y. (2017). Synthesis and applications of stimuli-responsive hyperbranched polymers. *Progress in Polymer Science,* 64, 114-153.

Wang, P., Liu, D., Jiang, S., Gu, X., & Zhou, Z. (2007). The direct chiral separations of fungicide enantiomers on amylopectin based chiral stationary phase by HPLC. *Chirality,* 19(2), 114-119.

Yamago, S. (2021). Practical synthesis of dendritic hyperbranched polymers by reversible deactivation radical polymerization. *Polymer Journal,* 53(8), 847-864.

Yamakawa, H., & Yoshizaki, T. (2016). *Helical Wormlike Chains in Polymer Solutions, 2nd ed.* Berlin, Germany: Springer.

Yoshizaki, T., Nitta, I., & Yamakawa, H. (1988). Transport-Coefficients of Helical Wormlike Chains .4. Intrinsic-Viscosity of the Touched-Bead Model. *Macromolecules,* 21(1), 165-171.